5004 *Chem. Mater.* **2009,** *21,* 5004–5006
DOI:10.1021/cm902413c

CHEMISTRY OF MATERIALS
Communication

Rapid, Facile Microwave-Solvothermal Synthesis of Graphene Nanosheets and Their Polyaniline Nanocomposites for Energy Strorage

A. Vadivel Murugan, T. Muraliganth, and A. Manthiram*

Electrochemical Energy Laboratory and Materials Science and Engineering Program, The University of Texas at Austin, Austin, Texas 78712

Received August 6, 2009
Revised Manuscript Received October 10, 2009

Graphene, a single layer of carbon atoms tightly packed into a two-dimensional (2D) honeycomb sp^2 carbon lattice, has attracted a great deal of attention in recent years because of its intriguing properties such as large thermal conductivity, superior mechanical properties, and unusual electronic properties.[1a,b] Moreover, graphene offers superior chemical stability, large surface-to-volume ratio, and a broad electrochemical window, which render it as an attractive electrode material for lithium ion batteries and electrochemical capacitors.[2a−c] Nevertheless, realization of several of these applications is still not feasible because large-scale production of graphene nanosheets remains a huge challenge. In recent years, various synthetic approaches have been pursued to prepare graphene nanosheets.[3a−c] Among the various strategies pursued, the reduction of graphite oxide (GO) is one of the most promising methods.[3d−f] However, the reduction of GO involves reaction with strong reducing agents like hydrazine or dimethylhydrazine at elevated temperatures (80 °C) for an extended period of 12−24 h or thermal treatment at elevated temperatures (1050 °C) in a vacuum/inert atmosphere. More recently, metal nanoparticles dispersed on graphene sheets have been prepared using hydrazine as a reducing agent in a domestic microwave oven.[3f] Unfortunately, the use of highly toxic and dangerously unstable hydrazine or dimethylhydrazine to reduce GO remains a serious challenge for large-scale production of graphene nanosheets.

Recognizing these difficulties, we present here for the first time a facile microwave-assisted solvothermal (MW-ST) reduction of exfoliated GO with nontoxic solvents to obtain "chemically modified graphene nanosheets" (GNS) within a short reaction time of 5−15 min at relatively low temperatures (180−300 °C). The MW-ST approach offers several advantages compared to the conventional solvothermal or hydrothermal methods.[4a,b] The MW-ST method centers on dielectric microwave heating of the reactants by transferring energy selectively to microwave absorbing polar solvents with a simultaneous increase in self-generated pressure inside the sealed reaction vessel, which shortens the reaction time from several hours to a few minutes with enormous energy savings and cleanliness. We also present here a decoration of the GNS produced with polyaniline (PANI) and an exploration of the graphene−PANI nanocomposites as electrode materials for lithium-ion batteries and supercapacitors.

GO prepared from graphite by the Hummer's method[5a] was dispersed in high boiling tetraethylene glycol (TEG, a polyol), and the yellow-brown colloidal suspension formed was subjected to MW-ST reduction at 300 °C. During the MW-ST process, the colloidal solution changed into black, confirming the reduction of GO to GNS. The MW-ST reduction of GO was also carried out at a lower temperature of 180 °C with various other polar solvents such as *N*,*N*-dimethyl formamide (DMF), ethanol, 1-butanol, and water, and the reduction process offered a black colloidal precipitate. The rapid absorption of microwave radiation by GO in polar solvents with a subsequent increase in temperature and pressure facilitate the reduction of GO while polyol, DMF, or supercritical water[5b] act as reducing agents under the solvothermal condition. We could also obtain stable graphene suspensions by the MW-ST heating of exfoliated GO suspension in an alkaline (NH_3 or NaOH) medium (pH ≈ 10) at 180 °C. In the basic medium, subsequent carboxyl termination occurred with the evidence of fast color change from yellow-brown to black during the MW-ST process as the exfoliated GO with negatively charged oxygen functional groups can undergo fast deoxygenation in strong alkaline solution.[5c]

Figure 1a−c shows the X-ray diffraction (XRD) patterns of pristine graphite, as-synthesized GO, and GNS obtained by the MW-ST reduction of colloidal GO in TEG at 300 °C. The substantial shift of the (002) reflection from 8.36 to 3.55 Å after the MW-ST processing of GO confirms the formation of graphene from GO. However, the interlayer spacing of the GNS produced is slightly higher than that of well ordered graphite (3.36 Å), suggesting the

(1) (a) Geim, A. K.; Novoselov, K. S. *Nat. Mater.* **2007**, *6*, 183. (b) Park, S.; Ruoff, S. R. *Nat. Nanotechnol.* **2009**, *4*, 217.
(2) (a) Yoo, E. J.; Kim, J.; Hosono, E.; Zhou, H. S.; Kudo, T.; Honma, I. *Nano Lett.* **2008**, *8*, 2277. (b) Stoller, M. D.; Park, S.; Zhu, Y.; An, J.; Ruoff, R. S. *Nano Lett.* **2008**, *8*, 3498. (c) Vivekchand, S. R. C.; Rout, C. S.; Subrahmanyam, K. S.; Govindaraj, A.; Rao, C. N. R. *J. Chem. Sci.* **2008**, *120*, 9.
(3) (a) Novoselov, K. S.; Geim, A. K.; Morozov, S. V.; Jiang, D.; Zhang, Y.; Dubonos, S. V.; Grigorieva, I. V.; Firsov, A. A. *Science* **2004**, *306*, 666. (b) Sutter, P. W.; Flege, J.-I.; Sutter, E. A. *Nat. Mater.* **2008**, *7*, 406. (c) Choucair, M.; Thordarson, P.; Stride, J. A. *Nat. Nanotechnol.* **2009**, *4*, 30. (d) Liu, N.; Luo, F.; Wu, H.; Liu, Y.; Zhang, C.; Chen, J. *Adv. Funct. Mater.* **2008**, *18*, 1518. (e) Tung, V. C.; Allen, M. J.; Yang, Y.; Kaner, R. B. *Nat. Nanotechnol.* **2009**, *4*, 25. (f) Hassan, M. A.; Abdelsayed, V.; Khder, S. R.; Abouzeid, K. M.; Terner, J.; Samy El-Shall, M.; Al-Resayes, S. I.; El-Azhary, A. A. *J. Mater. Chem.* **2009**, *19*, 3832.
(4) (a) Gerbec, J. A.; Magana, D.; Washington, A; Strouse, G. F. *J. Am. Chem. Soc.* **2005**, *127*, 15791. (b) Vadivel Murugan, A.; Muraliganth, T.; Manthiram, A. *J. Phys. Chem. C* **2008**, *112*, 14665.
(5) (a) Hummers, W. S.Jr.; Offeman, R. E. *J. Am. Chem. Soc.* **1958**, *80*, 1339. (b) Zhou, Y.; Bao, Q.; Tang, L. L.; Zhong, Y.; Loh., K. P. *Chem. Mater.* **2009**, *21*, 2950. (c) Fan, X.; Peng, W.; Li, Y.; Li, X.; Wang, S.; Zhang, G.; Zhang, F. *Adv. Mater.* **2008**, *20*, 4490. (d) Buchsteiner, A.; Lerf, A.; Pieper, J. *J. Phys. Chem. B.* **2006**, *110*, 22328. (e) Park, S.; An, J.; Jung, I.; Piner, R. D.; An, S. J.; Li, X.; Velamakanni, A.; Ruoff, R. S. *Nano Lett.* **2009**, *9*, 1593.

 Published on Web 10/16/2009

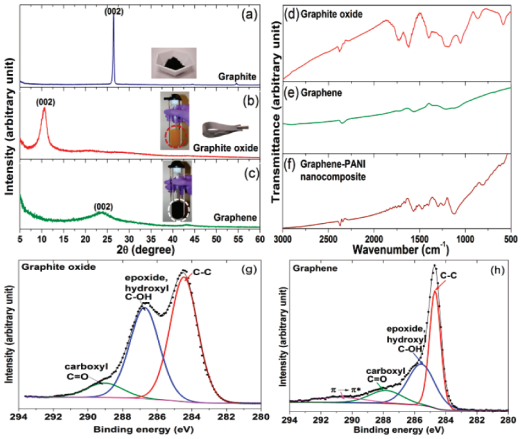

Figure 1. XRD patterns of (a) graphite, (b) GO, and (c) GNS, FTIR spectra of (d) GO, (e) GNS, and (f) graphene-PANI nanocomposite, and C 1s XPS spectra of (g) GO and (h) GNS.

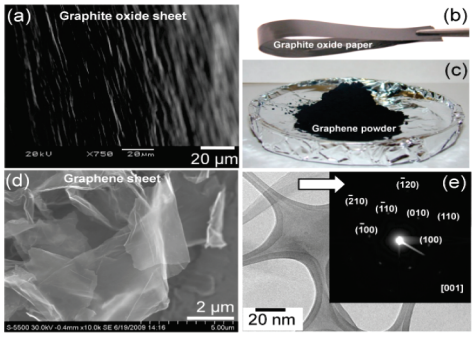

Figure 2. (a) SEM image of the cross-section of the GO paper, (b) photographic image of GO paper, (c) bulk quantity of GNS powder produced by the MW-ST process, (d) FE-SEM image of large micrometer size single paper-like GNS, and (e) bright field TEM image with the inset showing the electron diffraction pattern of optically transparent GNS.

presence of residual oxygen functionalities in the GNS. Nevertheless, the broad nature of the reflection indicates poor ordering of the sheets along the stacking direction, implying that the samples are composed of mostly single or few layers of GNS. Similarly, the GNS produced by the MW-ST reduction of GO at a lower temperature of 180 °C in TEG, DMF, ethanol, 1-butanol, and H_2O show interlayer spacings of, respectively, 3.62, 3.63, 3.84, 3.85, and 3.87 Å (Supporting Information Figure S1). Recognizing that a higher interplanar spacing may imply the presence of a higher concentration of residual oxygen functionalities, we can envision that the solvothermal reduction of GO in TEG and DMF is much more effective than that in ethanol, 1-butanol, or water. However, the residual solvent molecules present could also influence the interlayer spacing values.[5d] Also, the decrease in interplanar spacing on going from 180 to 300 °C in TEG (Supporting Information Figure S1) reveals that the solvothermal reduction of GO becomes more effective with increasing temperature and pressure. To provide further evidence for the formation of GNS from GO during the MW-ST process, we characterized the samples by Fourier transform infrared (FTIR) spectroscopy and X-ray photoelectron spectroscopy (XPS).

Figure 1d,e shows the FTIR spectra of GO and the reduction product obtained after the MW-ST process in TEG at 300 °C. The FTIR spectra of GO shows a strong absorption band at 1724 cm^{-1} due to the C═O stretching. It also exhibits bands around 1622 cm^{-1} due to aromatic C═C as well as bands due to carboxy C—O (1412 cm^{-1}), epoxy C—O (1232 cm^{-1}), and alkoxy C—O (1070 cm^{-1}) groups situated at the edges of the GO nanosheets as has been reported previously.[5e]After the MW-ST process, the intensity of the absorption band due to the C═O group (1724 cm^{-1}) decreases significantly, and the band at 1622 is absent. Instead, a new absorption band appears at 1562 cm^{-1}, which is attributed to the skeletal vibration of the graphene sheets. The FTIR data are similar to the data reported in the literature for samples obtained by the hydrazine reduction method.[5e] Also, the FTIR spectrum of the graphene-PANI nanocomposite (Figure 1f) shows the C═N and C═C stretching of the quinonoid and benzenoid units, respectively, at 1580 cm^{-1} and 1489 cm^{-1}. The bands at 1299 and 1241 cm^{-1} in Figure 1f are assigned to the C—N stretching of the benzenoid unit while the band at 1134 cm^{-1} is due to the quinonoid unit of doped polyaniline. Also, the peak at 809 cm^{-1} is associated with the C—C and C—H of the benzenoid unit. Figure 1g,h shows the C 1s XPS spectra recorded before and after subjecting the GO to the MW-ST process in TEG. After deconvolution, the C 1s spectrum of GO (Figure 1g) clearly shows the lower binding energy feature at 284.5 eV corresponding to C—C carbon and the higher binding energy feature at 286.8 eV followed by a shoulder at 289.1 eV, which is typically assigned to C—OH and C═O arising from epoxide, hydroxyl, and carboxyl functionalities.[5e] The XPS spectrum of graphene obtained after the MW-ST reduction process (Figure 1h), on the other hand, reveals that the intensities of the bands corresponding to carboxyl, epoxide, and hydroxyl functional groups are greatly reduced. Nevertheless, the sp^2 carbon network is retained in graphene as indicated by the C—C peak at 284.5 eV, and the remarkable $\pi \rightarrow \pi^*$ satellite peak around 290.8 eV is characteristic of aromatic or conjugated systems.[5c] In addition, based on the XPS data, the oxygen content decreases from 30.2% in GO (before the MW-ST process) to 8.3% in graphene (after the MW-ST process at 300 °C), which is similar to the data obtained with the graphene samples produced by the hydrazine reduction method.[5c,e] Thus, the XRD, FTIR, and XPS data demonstrate that the MW-ST process employed here with nontoxic solvents is efficient to produce GNS from graphite oxide.[5c]

Figure 2 shows the scanning electron microscopy (SEM), field emission SEM (FE-SEM), and transmission electron microscopy (TEM) data of GO and graphene obtained after the MW-ST process in TEG. While the SEM image and photograph in Figure 2a,b shows the paper-like character of GO, the FE-SEM image in Figure 2d shows the large (~15 × 5 μm) paper-like nanosheet morphology of graphene with slightly folded edges created during the ultrasonication of the colloidal dispersion. The bright field TEM image in Figure 2e shows the optically transparent graphene nanosheets, while the electron diffraction pattern reveals the well crystalline, large area of GNS, which may be attractive for electronic applications. AFM images (Supporting Information Figure S2) also reveal single or few layers of graphene sheets with a measured thickness of 1.5−2.5 nm.

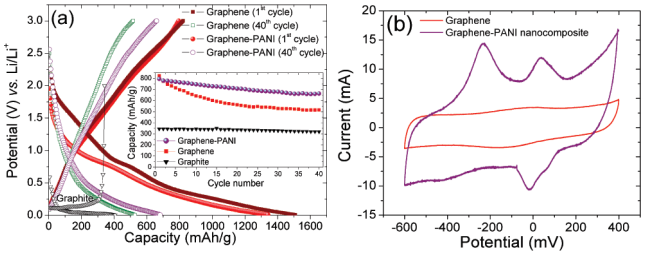

Figure 3. Comparative (a) charge−discharge profiles and cycalibility (inset) in lithium cells of graphite, GNS, and GNS-PANI at a constant discharge rate of C/15 and (b) cyclic voltammograms of GNS and GNS-PANI electrodes at a scan rate of 5 mV/s in 1 M H_2SO_4.

Figure 3a compares the first Galvanostatic charge−discharge profiles of commercial graphite and GNS at a constant discharge rate of C/15. The GNS offers much higher reversible capacity (~820 mA h/g) than the graphite anode (~340 mA h/g). During discharge (Li^+ insertion), a large part of the capacity occurs below 0.5 V (vs Li/Li^+) with a nearly plateau profile. This could involve the absorption of lithium on both sides of GNS, resulting in two layers of lithium per layer of graphene sheet to give Li_2C_6 as illustrated in Supporting Information Figure S3a. For a comparison, with a theoretical capacity of 372 mA h/g, the conventional graphite anode involves the insertion of one layer of lithium per carbon layer to give LiC_6 as shown in Supporting Information Figure S3a. The capacity above 0.5 V may be associated with a faradic capacitance either on the surface or on the edge planes of GNS.[6a] These kinds of lithium insertion/extraction mechanisms were first proposed for layer-type nanoporous carbons[6b] Although GNS offers much higher reversible capacity (Figure 3a) than graphite, it exhibits huge irrversibile capacity loss (685 mA h/g) in the first cycle due to electrolyte decomposition reactions occurring on the surface of GNS and the formation of the solid−electrolyte interfacial (SEI) layer.[6b] The GNS also exhibits capacity fade as seen in the inset of Figure 3a. However, the cyclability of our GNS produced by the MW-ST method is better than the cyclability data reported recently in the literature.[2a]

To improve the cyclability, we have decorated the GNS with a low-cost, conducting PANI. In addition to limiting the SEI layer formation, the electrochemically active PANI could help to enhance lithium-ion conduction and electron transport during cycling. As a result, the gaphene−PANI nanocomposite (90:10 wt %) offers a reversible capacity of ~800 mA h/g with considerably lower irreversible capacity loss (545 mA h/g) than pristine graphene. The nanocomposite also shows much improved cyclability with a capacity retention of 84% in 40 cycles compared to 63% retention for the pristine graphene. The significant improvement in capacity retention on decorating with a small amount (10 wt %) of PANI could be due to the modification of the graphene surface and pore structure by PANI.

In electrochemical capacitors (EC), capacitance can arise due to charge storage at the electrode−electrolyte interface (electrical double layer capacitor, EDLC) or fast redox reactions (pseudocapacitors).[7a] Carbon based materials have been particularly popular as electrodes for EDLC owing to their high surface area and electronic conductivity. However, their capacitance values are limited as high surface area does not always mean high capacitance due to the intricate involvement of pore size distribution.[7a,b] Remarkable improvements in performance have been achieved in recent years through the development of advanced nanostructured carbon materials, where ion desolvation occurs in pores smaller than the solvated ions, resulting in higher capacitance.[7c] Another attractive approach is to combine a pseudocapacitive material such as redox oxides, nitrides, and polymers with carbon.[7a] Considering the high surface area, excellent electrical conductivity, and multifunctional properties of graphene, we focused on nanocomposites consisting of graphene and PANI. Figure 3b shows the cyclic voltammograms (CV) of the pristine GNS and the graphene−PANI nanocomposite electrodes at a scan rate of 5 mV/s in 1 M H_2SO_4 electrolyte. The pristine GNS exhibits a rectangular shape CV that is characteristic of an EDLC with a specific capacitance of 100 F/g. On the other hand, the CV of graphene−PANI nanocomposite (50:50 wt %) shows a behavior characteristic of a combination of both EDLC and redox capacitance with a significantly enhanced overall specific capacitance of 408 F/g. The origin of the enhanced capacitance on combining the EDLC and pseudocapacitance is illustrated in Supporting Information Figure S3b. This nanocomposite strategy opens up possibilities to combine graphene with other redox pseudocapacitive materials like polythiophenes, MnO_2, and RuO_2 to enhance the energy density of ECs.

In summary, we have demonstrated a MW-ST process to produce GNS without the need for highly toxic chemicals with strong reducing properties or reducing gas atmospheres at high temperatures. The MW-ST process,taking advantage of both microwave radiation and solvothermal effect, produces GNS within a short reaction time of 5−15 min at < 300 °C, offering the possibilities of easy scale up and reduction in manufacturing cost. We have also demonstrated that the GNS thus produced and their nanocomposites with a conducting polymer like PANI exhibit good energy storage properties in lithium ion batteries and supercapacitors. We believe the facile synthesis approach presented here may pave the way for successfully employing graphene for microelectronics, photovoltaic, and energy storage and conversion applications.

Acknowledgment. This work was supported by the U.S. Department of Energy under Contract No. DE-AC02-05CH11231 and Welch Foundation Grant F-1254.

Supporting Information Available: Experimental procedure, XRD results, AFM images, and schematic illustrations of lithium storage in graphite and graphene and of the origin of enhanced capacitance (PDF). This material is available free of charge via the Internet at http://pubs.acs.org.

(6) (a) Yata, S.; Kinoshita, H.; Komori, M.; Ando, N.; Kashiwamura, T.; Harada, T.; Tanaka, K.; Yamabe, T. *Synth. Met.* **1994**, *62*, 153. (b) Xue, J. S.; Dahn, J. R. *J. Electrochem. Soc.* **1995**, *142*, 3668.

(7) (a) Simon, P.; Gogotsi, Y. *Nat. Mater.* **2008**, *7*, 845.(b) Conway, B. E. Electrochemcial supercapacitor: Scientific fundamentals and technological applications. Kluwer Academic/ Plenum: New York, 1999.(c) Huang, J.; Sumpter, B. G.; Meunier, V. *Chem. Eur. J.* **2008**, *14*, 6614.